The Cryosphere Discuss., 8, 1937–1972, 2014
www.the-cryosphere-discuss.net/8/1937/2014/
doi:10.5194/tcd-8-1937-2014


The Cryosphere Discussions Open Access



# Topographic control of snowpack distribution in a small catchment in the central Spanish Pyrenees: intra- and inter-annual persistence

**J. Revuelto, J. I. López-Moreno, C. Azorin-Molina, and S. M. Vicente-Serrano**

Instituto Pirenaico de Ecología, Consejo Superior de Investigaciones Científicas (IPE-CSIC) Departamento de Procesos Geoambientales y Cambio Global, Campus de Aula Dei, P.O. Box 13034, 50059, Zaragoza, Spain

Received: 3 March 2014 – Accepted: 2 April 2014 – Published: 15 April 2014

Correspondence to: J. Revuelto (jrevuelto@ipe.csic.es)

Published by Copernicus Publications on behalf of the European Geosciences Union.

## Abstract

In this study we analyzed the relations between terrain characteristics and snow depth distribution in a small alpine catchment located in the central Spanish Pyrenees. Twelve field campaigns were conducted during 2012 and 2013, which were years characterized by very different climatic conditions. Snow depth was measured using a long range terrestrial laser scanner and analyses were performed at a spatial resolution of 5 m. Pearson's $r$ correlation, multiple linear regressions and binary regression trees were used to analyze the influence of topography on the snow depth distribution. The analyses were used to identify the topographic variables that better explain the snow distribution in this catchment, and to assess whether their contributions were variable over intra- and inter-annual time scales. The topographic position index, which has rarely been used in these types of studies, most accurately explained the distribution of snow accumulation. Other variables affecting the snow depth distribution included the maximum upwind slope, elevation, and northing (or potential incoming solar radiation). The models developed to predict snow distribution in the basin for each of the 12 survey days were similar in terms of the most explanatory variables. However, the variance explained by the overall model and by each topographic variable, especially those making a lesser contribution, differed markedly between a year in which snow was abundant (2013) and a year when snow was scarce (2012), and also differed between surveys in which snow accumulation or melting conditions dominated in the preceding days. The total variance explained by the models clearly decreased for those days on which the snow pack was thinner and more patchily distributed. Despite the differences in climatic conditions in the 2012 and 2013 snow seasons, some similarities in snow accumulation patterns were observed.





TCD
8, 1937–1972, 2014

## 1 Introduction

Assessing the snow distribution in mountain areas is important because of the number of processes in which snow plays a major role, including erosion rates (Pomeroy and Gray, 1995), plant survival (Keller et al., 2000; Wipf et al., 2009), soil temperature and moisture (Groffman et al., 2001), and the hydrological response of mountain rivers (Bales and Harrington, 1995; Barnett et al., 2005; Liston, 1999; Pomeroy et al., 2004). As mountain areas are highly sensitivity to global change (Beniston, 2003), snow accumulation and melting processes are likely to be subject to marked changes in coming decades, affecting all processes influenced by the presence of snow (Caballero et al., 2007; López-Moreno et al., 2011, 2012b; Steger et al., 2012). For these reasons, much effort has been devoted to understanding the main factors that control the spatial and temporal dynamics of snow (Egli et al., 2012; López-Moreno et al., 2010; ; Mott et al., 2010; Schirmer et al., 2011).

One of the main difficulties in snow studies is obtaining reliable information of the variables that describe snow distribution, including snow depth (SD), snow water equivalent (SWE) and snow covered area (SCA). Manual measurements have traditionally been used to provide information on the distribution of snowpack, with different sampling strategies having been applied at various spatial scales (Jost et al., 2007; López-Moreno et al., 2012a; Watson et al., 2006). However, manual sampling is not feasible for large areas because of the time involved, especially when SWE measurements are also acquired. In the last decade the use of airborne laser scanners (ALS) (Deems et al., 2006) and terrestrial laser scanners (TLS) (Prokop, 2008), both of which are based on LiDAR (laser imaging detection and ranging) technology, have provided for major advances in obtaining data on the SD distribution at unprecedented spatial resolutions. These developments have enabled studies of several factors that in the past have been only marginally considered, including scaling issues (Fassnacht and Deems, 2006; Mott et al., 2011; Schirmer and Lehning, 2011; Trujillo et al., 2007), the detailed dynamics of snow accumulation and ablation (Grünewald et al., 2010; Schirmer et al.,





TCD
8, 1937–1972, 2014



Title Page
Abstract Introduction
Conclusions References
Tables Figures
◀ ▶
◀ ▶
Back Close
Full Screen / Esc
Printer-friendly Version
Interactive Discussion

2011; Scipión et al., 2013), and snow transport processes (Mott et al., 2010). In addition, the high density measurements provided by LiDAR technologies are a valuable resource for detailed investigation of the linkage between snow distribution and topography. In the past, this linkage has mostly been studied using manual measurements, and hence with generally limited spatial and temporal resolution (López-Moreno et al., 2010).

Previous studies have highlighted the marked control of topography on snow distribution in mountain areas (Anderton et al., 2004; Erickson et al., 2005), and the importance of vegetation and wind exposure (Erxleben et al., 2002; Trujillo et al., 2007). The most commonly used approach has been to develop digital elevation models (DEM) that describe the spatial distribution of elevation, from which other terrain variables are derived including slope, terrain aspect, curvature, wind exposure or sheltering, and potential solar radiation. This enables to analyze the linear or non-linear relation of these variables to punctual SD or SWE values to be established (Grünewald et al., 2010; Schirmer et al., 2011). Various statistical methods have been applied for this purpose, including linear regression models (Fassnacht et al., 2003; Hosang and Dettwiler, 1991), generalized additive models (GAM) (López-Moreno and Nogués-Bravo, 2005), and binary regression trees (BRT) (Breiman, 1984) which have been widely applied in a diversity of regions (Elder et al., 1991; Erxleben et al., 2002; McCreight et al., 2012).

The extent to which topographic variables explain snow distribution can change during the snow season; the variability of terrain characteristics can drive processes related to the spatial variability of snow accumulation (snow blowing, terrain curvature) (Lehning et al., 2008), or affect the energetic exchange between terrain and the snowpack (temperature, incoming solar radiation), so the importance of topographic variables is modified during the season (Molotch et al., 2005). In addition, during a snow season the terrain changes markedly (is smoothed) by snow accumulation (Schirmer et al., 2011). However, few studies have systematically analyzed the intra- and interannual persistence of the relation between snow distribution and topography. Recent





TCD
8, 1937–1972, 2014

studies have assessed whether the influence of topography is constant among different years; e.g. the similarities observed at the end of the accumulation season (Schirmer and Lehning, 2011; Schirmer et al., 2011), or the consistent fractal dimensions in two analyzed years (Deems et al., 2008); in both cases there was a relation with the dominant wind direction, which highlights the predictive ability of topographic variables.

The main focus of this study was to assess the influence of topography on the spatial distribution of snowpack and its evolution over time. The high temporal and spatial density of the dataset collected during the study enabled analysis of the main topographic factors controlling snow distribution, and assessment of whether topographic control of the snowpack varied during the snow season and between years having very contrasting climatic conditions. For this purpose, we conducted 12 surveys over 2012 (6) and 2013 (6) in a small mountain catchment representing a typical subalpine environment in the central Spanish Pyrenees, and obtained high resolution SD measurements using LIDAR technology using a TLS.

## 2 Study area and snow and climatic conditions

The Izas experimental catchment (42°44′ N, 0°25′ W) is located in the central Spanish Pyrenees (Fig. 1). The catchment is on the southern side of the Pyrenees, close to the main divide (Spain–France border), in the headwaters of the Gallego River valley, and ranges in elevation from 2000 to 2300 m a.s.l. The catchment is predominantly east-facing, with some areas facing north or south, and has a mean slope of 16°. There are no trees in the study area, and the basin is mostly covered by subalpine grasslands dominated by Festuca eskia and Nardus stricta, with rocky outcrops in the steeper areas; flat, concave and convex areas occur in the basin.

The climatic conditions are influenced by the proximity of the Atlantic Ocean, with the winters being humid compared with zones of the Pyrenees more influenced by mediterranean conditions. The mean annual precipitation is 2000 mm, of which snow accounts for approximately 50 % (Anderton et al., 2004). The mean annual air temper-





TCD
8, 1937–1972, 2014

ature is 3 °C, and the mean daily temperature is < 0 °C for an average of 130 days each year (del Barrio et al., 1997). Snow covers a high percentage of the catchment from November to the end of May.

The two years analyzed in the study represent climatic extremes during recent decades. Severe drought occurred during 2012, leading to snow accumulation well below the long-term average. The thickness of the snowpack during winter in this year was less than the 25th percentile of the available historical data series (1996–2011) (Fig. 2). Only at the end of spring did late snowfall events increase the amount of snow, but this rapidly melted. The opposite occurred in 2013, which was a year in which the deepest snowpack and the longest snow season of recent decades were recorded. Winter and spring in 2013 were extremely humid, with temperatures mostly between the 25th and 75th percentiles of the historical series. Snow depth accumulation was very high between February and June (exceeding the 75th percentile); in some areas of the basin it lasted until late July, which is one month longer than in most of the preceding years for which records are available.

## 3 Data and methods

### 3.1 Snow depth measurements

During the study period high resolution SD maps were generated using a long range TLS (Riegl LPM-321), which enables safe acquisition of SD information with short acquisition times from remote areas, compared with measurements obtained manually. This technique has been extensively tested (Prokop et al., 2008; Revuelto et al., 2014; Schaffhauser et al., 2008), and systematically applied to the study of snow distribution in mountain terrain (Grünewald et al., 2010; Schirmer and Lehning, 2011; Schirmer et al., 2011). In a previous study the mean absolute error in the most distant areas of the catchment was less than 10 cm (Revuelto et al., 2014), which is consistent with errors reported in previous studies (Prokop, 2008).

TLS provides high resolution three dimensional information on the terrain. Nevertheless, error sources need to be considered because they can have large effects on the measurements. To reduce the influences of TLS instability (which leads to misalignment with reference points) and atmospheric change, a well-defined protocol must be applied. The protocol applied in this study for generating high resolution SD maps with a 1 m cell size was described by Revuelto et al. (2014). The methodology was based on differences between DEMs obtained with snow coverage in the study area and a DEM taken at 18 July 2012, when the catchment had no snow cover. Twelve snow depth maps at a spatial resolution of 5 m were generated for the 2012 and 2013 snow seasons (Fig. 3). In each year three surveys were undertaken from February to April during the snow accumulation period (2012: 22 February, 2 April, 17 April; 2013: 17 February, 3 April, 25 April), and three were undertaken from May to June in the snowmelt period (2012: 2, 14 and 24 May; 2013: 6, 12 and 20 June). The average SD and SCA, and the maximum SD are shown in Table 1.

### 3.2 Digital elevation model and topographic variables

From the two scan stations (Revuelto et al., 2014) located in the study area (Fig. 1), 86 % of the total area of the catchment was surveyed using TLS at an initial spatial resolution of 1 m grid size. Some of the predictor variables cannot be calculated where data gaps occur in the DEM (e.g. the topographic position index), and others require a DEM with a greater surface than the area scanned during the study (e.g. to calculate the potential solar radiation, including the shadow effect from surrounding topography, or to calculate the maximum upwind slope parameter). Thus, a DEM having a 5 m grid-size, available from the Geographical National Institute of Spain (Instituto Geográfico Nacional, www.ign.es), was combined with the snow-free DEM obtained using the TLS resampled from 1 m to 5 m resolution (the empty raster of the Geographical National Institute was used for the resampling, averaging all values within each cell). The 1 m grid-size SD maps were also resampled to 5 m to enable matching of the two different data sources.

To characterize the terrain characteristics, eight variables were derived from the final DEM, including: (i) elevation (*Elevation*), (ii) slope (*Slope*), (iii) curvature (*Curvature*), (iv) potential incoming solar radiation under clear sky conditions (*Radiation*), (v) easting exposure (*Easting*), (vi) northing exposure (*Northing*), (vii) the topographic position index (*TPI*) and (viii) maximum upwind slope (*Sx*).

*Elevation* was obtained directly from the DEM, while the other variables were calculated using ArcGIS10.1 software. This calculates *Slope* as the maximum rate of change in value from a specific cell to that of its neighbors, and C*urvature* is determined from the second derivative of the fitted surface to the DEM. *Radiation* was obtained using the algorithm of Fu and Rich (2002) and reported in watts hour per square meter based on the average conditions for the 15 day period prior to each snow survey. This measure provided the relative difference in the extraterrestrial incoming solar radiation among areas of the catchment for a given period under given topographical conditions (Fassnacht et al., 2013). *Easting* and *Northing* exposure were calculated directly as the sine and cosine of the angle between direction north and the maximum slope line of the terrain, respectively. It provided information on the east (positive)/west (negative) exposure and the north (positive)/south (negative) exposure.

The *TPI* provided information on the relative position of a cell in relation to the surrounding terrain at a specific spatial scale. Thus, this index compared the elevation of each cell with the average cell elevation at various radial distances (Weiss, 2001). For each pixel the *TPI* was calculated for 10, 15, 25, 50, 75, 100, 125, 150 and 200 m radial distances.

For specific wind directions, the maximum upwind slope parameter (*Sx*; Winstral et al., 2002) provided information on the exposure or sheltering of individual cells at various distances, resulting from the topography. Rather than considering the contribution from all directions at a specific location, adding all the *Sx* values for all directions for each cell (Winstral et al., 2002), or only analyzing the dominant wind directions (Molotch et al., 2005), *Sx* values for eight directions were selected and directly related to the SD. The directions were: 0° for north (N), 45° for northeast (NE), 90° for east (E),





TCD
8, 1937–1972, 2014

135° for southeast (SE), 180° for south (S), 225° for southwest (SW), 270° for west (W), and 315° for northwest (NW). For *Sx* the searching distances (Winstral et al., 2002) considered were 100, 200, 300 and 500 m. These distances were selected to enable assessment of the range at which *Sx* exhibited greatest control on SD dynamics, as has occurred in previous studies (Schirmer et al., 2011; Winstral et al., 2002).

### 3.3 Statistical analysis

The 12 SD maps at 5 m spatial resolution were related to each of the topographic variables considered (including the 40 *Sx* combinations, and the 9 distances for *TPI*). The large number of cells for which snow depth data were available enabled robust correlations between topography and snow distribution to be obtained, and provided a very large dataset for training and validation of the SD distribution models.

Pearson's *r* coefficients were obtained between SD and each topographic variable. Given the large amount of data for each sample, the degrees of freedom for the correlation analyses were very high. For this reason we followed a Monte Carlo procedure, in which 1000 random samples of 100 SD cases were extracted from the entire dataset and correlated with topographic variables. A threshold 95 % confidence interval ($\alpha < 0.05$) was used to assess the significance of correlations ($r = \pm 0.197$, based on 100 cases) (Zar, 1984). The spatial scales of *Sx* (200 m) and *TPI* (25 m), for which SD showed a higher correlation, were selected for further analysis.

To assess the explanatory capacity when all topographic variables were considered simultaneously, two statistical models were used: (1) multiple linear regressions (MLRs) and (2) binary regression trees (BRTs). A wide variety of regression analyses for interpretation of much more complex spatial data are available with greater capacity than MLRs and BRTs to deal with spatial autocorrelation issues and the non-linear nature of the relationship between predictors and the response variable (Beale et al., 2010). However, in this study we used MLRs and BRTs because these methods have been and are still widely used in snow studies, and because both enable to isolate accurately





TCD
8, 1937–1972, 2014

the weight of each independent variable within the model, which was the main objective of this research, rather than deriving models with maximum predictive capacity.

1. *Multiple linear regression* estimates the linear influence of topographic variables on SD. Despite its simplicity and the rather limited capability under nonlinear conditions (López-Moreno et al., 2010), MLR was used to quantify the relative contribution of each variable to the entire SD distribution model. SD was calculated from the topographic variables at a specific location for a given day using Eq. (1):

   $$z_i = b_1x_1 + b_2x_2 + \ldots + b_nx_n \quad (1)$$

   where $z_i$ is the predicted SD value; $b_1, b_2, \ldots, b_n$ are the beta standardized coefficients of the model; and $x_1, x_2, \ldots, x_n$ are the independent (topographic) variables. We followed a stepwise mode to avoid redundancy and collinearity problems among independent variables. The threshold for a variable to enter in the model was set at $\alpha < 0.05$. We used the beta (standardized) coefficients to determine the contribution of each variable to the model. Twelve MLR models were obtained, one for each survey day. To avoid problems of over-fitting as a consequence of the large numbers of available cases (Hair et al., 1998), samples of 1000 cases were randomly selected from the entire dataset; 5000 cases were used for model validation.

2. *Binary regression trees* have been widely used to model snowpack distribution from topographic data (Erxleben et al., 2002; Molotch et al., 2005). These are nonparametric models that recursively split the data sample, based on the predictor variable that minimizes the square of the residuals obtained (Breiman, 1984). One BRT was created for each sampling date. The BRTs were run until a new split was not able to account for 1 % of the explained variance, or when a node had less than 500 cases; a maximum of 15 terminal nodes was set, to reduce tree complexity. As there were no over-fitting problems associated with sample size,





TCD
8, 1937–1972, 2014

15 000 cases were used to grow the trees and 5000 cases were used for validation. By scaling the explained variance of each variable introduced into each BRT (based on the % of the total explained variance by the BRT), we were able to compare the relative importance of each topographic variable between the different models.

Coefficients of determination ($r^2$) and Willmott's $D$ statistic were used to assess the ability of each model to predict snow depth over an independent random sample of 5000 cases. Willmott's $D$ was determined using Eq. (2) (Willmott, 1981):

$$D = 1 - \frac{\sum_{i=1}^{N}(P_i - O_i)}{\sum_{i=1}^{N}(|P_i - \bar{O}| + |O_i - \bar{O}|)^2} \tag{2}$$

where $N$ is the number of observations, $O_i$ is the observed value, $P_i$ is the predicted value, and $\bar{O}$ is the mean of the observed values. The index ranges from 0 (minimum) to 1 (maximum) predictive ability.

## 4 Results

### 4.1 Single correlations

Figure 4 shows the correlation between SD and $Sx$ for the eight wind directions at a distance of 200 m (identified as the best correlated searching distance). Despite differences in magnitude, the correlations for surveys carried out at the beginning of the season in each year showed that SD was clearly affected by N and NW wind directions. This was particularly evident in 2013, as the correlation values were higher. The contribution of N and NW wind directions is clearly evident for the surveys on 17 February 2013 and 3 April 2013 (Fig. 3), when greater SD was recorded in the leeward slopes from a northerly direction (upper areas of the maps). In the two years of the study a correlation with W and SW wind directions was observed to increase progressively





TCD
8, 1937–1972, 2014

during the snow season. In 2013 this phenomenon was less marked because of the greater SD accumulation at the beginning of the snow season accompanied with N direction winds, which resulted in only moderate changes in the *Sx* for the most strongly correlated wind directions. It was also observed that in both study years once the snow had started to melt (the last three surveys in each season) the snow distribution did not change in relation to *Sx* directions.

Correlations between the most correlated *Sx* direction for each day and SD were compared with correlations between SD and the other topographic variables (Fig. 5). This showed that *Sx* had one of the greatest coefficient of correlation with SD (range 0.18–0.53). The correlations were higher during the accumulation periods, especially in the 2013 snow season, with a reduction in correlations values occurring during the melt period at the end of each snow season.

The *TPI* at 25 m showed the highest correlation with SD for nearly all of the 12 sampled days. During 2012 the mean correlation values ranged from −0.5 to −0.6 for those surveys during which snow accumulation dominated in the days preceding the surveys. The *r* values were closer to the significance level (−0.197) for the surveys where the preceding days were dominated by melting conditions (14 and 24 May). In 2013, the *TPI* was more highly correlated with SD than in 2012, with Pearson's *r* coefficients $< -0.6$ for all survey days. *Curvature* also had a high correlation with SD, and similar to *TPI* with a 25 m searching distance was significantly correlated on all the survey dates, but unlike the *TPI*, the correlation of *Curvature* with SD did not decrease during the snowmelt periods. The significant correlations of *TPI* and *Curvature* with SD highlight the importance of terrain curvature on the SD distribution. The importance of terrain curvature at different scales for SD distribution is clearly evident in Fig. 3, which shows that higher SD values were usually found for concave areas, which showed snow presence until the end of each snow season.

The correlation between *Elevation* and SD varied among survey days (Fig. 5). The correlations were usually positive, but only statistically significant (or approaching significance) for days when melting dominated (the last two surveys in 2012 and 2013).





TCD
8, 1937–1972, 2014

*Slope* was relatively weakly correlated with SD during the 2012 snow season. In 2013 the correlation was greater, and was statistically significant on some days. As with *Elevation*, the correlation between *Slope* and SD was variable between the two study years, and showed a similar temporal pattern to *Easting*, probably because of the presence of steeper areas on the east-facing slopes.

The correlation between *Northing* and SD was rarely statistically significant, was highly variable, and contributed to explaining SD in a very different ways in 2012 and 2013. In 2012 no correlation between SD and *Northing* was found during the accumulation period, but during the melting period a slight positive correlation was observed, as snow remained longer on north-facing slopes. The 2013 snow season started with a large precipitation event dominated by strong winds from a northerly direction, leading to high levels of snow accumulation on the south-facing slopes. This explains the strong and statistically significant negative correlation of SD with *Northing* for 17 February 2013. This event influenced the rest of the season (as evident in Fig. 4 in 2013), but a progressive decrease in its influence was evident for the following survey days. *Radiation* had an almost opposite influence on SD to that observed for *Northing*. During the melting period in each year the Pearson's $r$ correlation between SD and *Radiation* was negative, indicating a thinner snowpack on the most irradiated slopes; the relation was statistically significant at the end of the 2013 snow season.

## 4.2 Multiple Linear Regression and Binary Regression Tree models

Figure 6 shows the Willmott's $D$ values and the coefficients of determination ($r^2$) obtained in the comparison of observed and predicted values using MLRs and BRTs for an independent dataset (5000 cases) reserved for validation. The MLRs produced $r^2$ values ranging from 0.27 to 0.65 and Willmott's $D$ values ranging from 0.63 to 0.88, while the BRTs produced $r^2$ values ranging from 0.43 to 0.58 and Willmott's $D$ values ranging from 0.74 and 0.85. For both methods the relationship between the observed and predicted values was stronger for 2013. Accuracy decreased at the end of the snow season, when the snowpack was mostly patchy across the basin; this was particularly the case for the end of the 2012 season. Overall, the performance of the MLRs was more variable than that of the BRTs, which were more constant amongst the various snow surveys. For those days on which the models were most accurate in predicting SD variability, the MLRs showed slightly better scores than the BRTs. However, for days on which the accuracy between predictions and observations was lower, the BRTs provided better estimates than the MLRs. For 2012, slightly better results were obtained using MLRs, while the opposite occurred in 2013. Nevertheless, only large differences in the accuracy of each model were evident by the end of 2012 snow season, in the two last surveys, which were characterized by thin and patchy snowpack. In general, there was good agreement between the models for each survey day, so results obtained with each model could be compared.

As shown for single correlations, the *TPI* variable explained most of the variance in MLR models developed for all analyzed days (Table 2). The contribution of the other variables varied markedly among surveys, particularly when the two years were compared. In most cases, *Elevation* was the second most important variable explaining the SD distribution in 2012, followed by *Sx* and *Slope*. The other variables made a much smaller contribution, or were not included in the models. The contribution of *Elevation* was much less in 2013, and it was not included in three of the six surveys, whereas in 2012 it was included in all surveys. For the entire 2013, *Sx* was the second most important variable, followed by *Curvature*, which had an almost negligible influence in 2012. *Northing* was only included in the models for the surveys carried out during periods dominated by snow accumulation, and was not included in the models during the periods dominated by melting.

Figure 7 shows two examples of BRTs, obtained for the days 2 May 2012 (upper panel) and 3 April 2013 (bottom panel), which accounted for the largest amount of snow accumulation in each of the two years. The variable *TPI* determined the first branching point, and this occurred in the majority of the trees obtained (not shown). After the first branching, other variables were significant in the model, including *Sx*





TCD
8, 1937–1972, 2014

and *TPI* for 2 May 2012, and *Sx* and *Northing* for 3 April 2013, demonstrating the importance of these variables in the subsequent branching of the trees.

The relative importance (scaled from 0 to 100) of each topographic variable in each BRT is shown in Table 3. This shows that *TPI* was the first most important variable explaining SD for all survey days. For the 2012 snow season, *TPI* explained more than 67 % of the total explained variance in all BRTs, and 75 % during the accumulation period (the first three surveys). Thus, for most of the survey days the variance explained by the other variables was < 30 %. The second most important variable explaining the SD distribution in 2012 differed amongst the survey days. Thus, *Sx* was the second most influential variable during May (except for 24 May 2012), following the largest snowfall in the season (which occurred the 1 May 2012), and *Elevation* was the most important variable in the other surveys during 2012. *Northing* also had an evident influence during the two first surveys of the year, but subsequently had minimal explanatory capacity, as was the case for all the other variables. In 2013 *TPI* was also the main contributor to the total explained variance, exceeding 50 % for almost all survey days, and approaching or > 70 % during the snowmelt period. The influence of *Sx* was more important in 2013 than in the previous year. At the beginning of 2013 the contribution of *Sx* to the total explained variance was almost 46 %, and remained > 20 % for the rest of the snow season; an exception was the last survey, when melting dominated and its effect declined to 12 %. When snow was not mobilized for long periods by wind, the SD distribution was more dependent on variables related to terrain curvature (*TPI* and *Curvature*). During 2013, *Elevation* contributed approximately 5 % to the total explained variance during the entire snow season. *Northing* made a significant contribution to the model (14.7 %) on only one day (3 April 2013), and a much smaller contribution on the following survey day (25 April 2013). Where included in the BRTs, the other variables (*Easting*, *Radiation*) made no, or only minor, contributions to the total explained variance.





TCD
8, 1937–1972, 2014

## 5 Discussion

The distribution of snow in mountain areas is highly variable in space and time, as was shown for the Izas experimental catchment during two consecutive years. Many meteorological and topographic parameters affect the snow distribution and its evolution through time. In this context, we demonstrated that topography was a major controlling factor affecting SD in a subalpine catchment, and showed that its effect evolved during the snow accumulation and melting periods over two years having highly contrasting climatic conditions and levels of snow accumulation.

There have been many studies of the spatial distribution of SD in mountain areas (Anderton et al., 2004; Erickson et al., 2005; López-Moreno et al., 2010; Mccreight et al., 2012), but there are very few datasets that have enabled investigation of the intra- and inter-annual occurrence of topographic control on the snowpack distribution. The results of previous research have highlighted the difficulties in fully explaining the distribution of snow in complex mountainous terrain. In addition, the results have differed among studies, and suggest that different variables govern the distribution of snowpack among areas as consequence of their differing characteristics and geographical settings, including surface area and altitudinal gradients, the importance of wind redistribution, the presence or absence of vegetation, and the topographic complexity (Grünewald et al., 2013).

Most of the topographic variables investigated in this study have been included in previous studies, including *Elevation, Slope, Radiation, Curvature* and *Sx.* Other variables, in particular *TPI*, have received little attention in previous research (López-Moreno et al., 2010). We showed that *TPI* at a scale of 25 m had the greatest capacity to explain the SD distribution in the study catchment. *Curvature* (which refers to a small spatial scale of terrain curvature) was also highly correlated with the SD distribution, but not as highly as *TPI*, reinforcing the importance of considering terrain curvature at various scales in explaining the SD distribution in mountain environments. The correlation between snowpack and the *TPI* decreased during melting periods, whereas the





TCD
8, 1937–1972, 2014

Topographic control of snowpack distribution

J. Revuelto et al.

correlation with *Curvature* remained constant. This suggests that snow remains longer in small, deep concavities, but melts faster in wider concave areas that were identified by the 25 m *TPI* scale. This effect was evident at the end of the snow season, when snow was present only in deep concavities, as shown in Fig. 3. To explain the snow distribution, Anderton et al. (2004) compared the relative elevation of a cell with the terrain over a 40 m radius, and observed that this had a major role on SD distribution, what reinforces curvature importance at different scales.

The maximum upwind slope (*Sx*; Winstral et al., 2002) has also been identified as a key variable explaining snow distribution, improving the results obtained when it is introduced into models. Our results are consistent with those of other studies that have shown that the optimum searching distance for correlating *Sx* with the SD distribution is 200 m (Molotch et al., 2005; Schirmer et al., 2011). The Izas experimental catchment does not have a clearly dominant wind direction. For this reason, the *Sx* preferred direction for each date was selected, and showed that there were intra-annual shifts in the most highly correlated direction. The change in the most important *Sx* direction was similar between the 2012 and 2013 snow seasons; it started with a northerly component and evolved to a dominant westerly direction. We also found a decrease in the correlation between *Sx* and the snow distribution at the end of each snow season, when melting conditions dominated; this is consistent with the findings of previous studies (Winstral and Marks, 2002).

Only for two days (22 February 2012 and 2 April 2012) was there no (or a minor) contribution of *Sx* to SD, according to the BRTs and MLRs. On these days *Northing* was introduced into the models, and was found to explain some of the variance of *Sx* from northerly direction (the best correlated direction for these days; Fig. 4).

Although *Elevation* has been found to largely explain the snow distribution in areas having marked altitudinal gradients (Elder et al., 1998; Erxleben et al., 2002; Molotch and Bales, 2005) in our study no strong association was found between SD and *Elevation*, with the only significant correlations occurring during the snowmelt period. This is because of the low elevation range of the study area (300 m). During the accumulation period the entire catchment is generally above the freezing height. However, during spring the 0 °C isotherm shifts to higher elevations, which may lead to different melting rates within the basin. Despite the relatively weak correlation between *Elevation* and SD, this variable was introduced as a predictor in the MLRs and BRTs for most of the days analyzed, as López-Moreno et al. (2010) reported that elevation was of increasing importance as the grid size increased, and Anderton et al. (2004) reported its importance in the same study area. The results of the present study also suggest the importance of *Elevation*, particularly when considered in combination with other topographic variables.

*Slope* was only a weak explanatory factor for snow distribution, probably because the slope in most of the catchment is not sufficient to trigger gravitational movements including avalanches and slushes during the snowmelt period, which could thin the snowpack on the steepest slopes (Elder et al., 1998).

*Radiation*, *Northing* and *Easting* showed no close correlation with the snowpack distribution; their relationships with SD were variable over time, with statistically significant correlations occurring on some days and only weak correlations on other days. The results suggested that *Radiation* and *Northing* (which showed almost opposite patterns) may be related to SD for two different reasons. During the accumulation period in 2013 heavy snowfalls associated with northerly winds led to the accumulation of deep snow on south-facing (more irradiated) surfaces, whereas during the snowmelt period the greater exposure of the southern slopes to solar energy led to a positive (negative) correlation with *Northing* (*Radiation*). This phenomenon was also observed by López-Moreno et al. (2013), using a physically-based snow energy balance model in the same study area. Another effect observed with *Northing* was the contributions of this variable to the MLRs and BRTs only for survey days corresponding to snow accumulation conditions, while in the three last surveys of both years *Northing* was not introduced in the models. This result indicates there was consistency between the two analysis years with respect both models. Although *Radiation* did not show a significant correlation with SD during accumulation periods, when the surveys were closer to the snowmelt





TCD
8, 1937–1972, 2014

period the negative correlation of this variable with SD was much more evident, possibly due to the increase of the difference in the energetic exchange between the sun exposed and shaded areas. Terrain aspect (mainly *Northing*) and *Radiation* during winter were not found to have high explanatory capacity relative to the other variables. Nevertheless, these are useful indicators of the general patterns of snow accumulation processes because of their relation to the dominant *Sx* directions. Thus, *Northing* and *Radiation* are equivalent variables in explaining the SD distribution. More importantly, during winter they were more related to the accumulation patterns resulting from wind redistribution, whereas in spring they were associated with the unequal distribution of solar radiation, which leads to higher melting rates on the most irradiated slopes. Other studies that have compared *Northing* and *Radiation* have obtained better simulations when solar radiation was used (Molotch et al., 2005).

The MLRs and BRTs provided reasonably high accuracy scores when observed and predicted SD data were compared. The scores were slightly better than reported in previous research using similar methods, especially as they were obtained from a dataset independent of that used to create the models. One reason for the improvement may be the use of the *TPI* as a SD predictor, as this variable has not been considered in previous studies. For the 12 survey days the *TPI* had the greatest explanatory capacity in both approaches. However, based on comparison of the different dates and surveys, the other variables made more varying contributions, as a result of the different roles they play during the snow accumulation and melting periods, and the wind conditions during the main snowfall events. The models had less capacity to explain spatial variability of the snowpack when the snow was thinner and patchy. The BRT and MLR approaches were consistent with respect to error estimates. The results obtained using each approach were comparable, so the trends in the variable ranking for both models for each survey day were very similar. Only during conditions of snow scarcity did the BRT approach demonstrate better capability to relate SD to topography. This is probably a consequence of the greater capacity of BRTs to take account of the nonlinear response of the snowpack to topography, and the occurrence of sharp thresholds typical of days when the snowpack is patchy (López-Moreno et al., 2010; Molotch et al., 2005).

The similarity of the models obtained for 2012 and 2013 suggests a consistent interannual distribution of the snow pack in the catchment; the areas of maximum SD and the location of snow free zones were consistent between both years of the study. The detected spatial consistency of snowpack has implications for soil dynamics and plant cycles, because some parts of the basin will tend to remain free of snow cover during longer periods favoring the presence of temporary frozen soils, and reducing the isolation effect of snowpack to the plants (Keller et al., 2000; Pomeroy and Gray, 1995). Moreover, it suggests that the information acquired from TLS during several years could be useful to design long-term monitoring strategies of SD in the basin based on few manual measurements in representative points according their terrain characteristics.

## 6 Conclusions

Topographic variables related to terrain curvature were shown to contribute more to explaining snow distribution than other variables. In particular, the *TPI* at a 25 m searching distance was the major variable explaining SD in the Izas experimental catchment. This suggests the importance of including this index in future snow studies, and the need to establish the best searching distance for relating this variable to SD distribution at other study sites. The maximum upwind slope at a searching distance of 200 m was also an important variable explaining the SD distribution. However, its influence varied markedly between years and surveys, depending of the specific wind conditions during the main snowfall events. The influence of the other topographical variables on the spatial distribution of SD was less, and showed greater intra- and inter-annual variability. The results from BRTs and MLRs models were consistent, and the explanatory capacities of the main variables were very similar for all surveys. This suggests that the effect of topography on snow distribution has relatively high intra- and inter-annual





TCD
8, 1937–1972, 2014

consistency in the study catchment. Several interesting temporal evolutions during the two snow seasons were found in the relation of some topographic variables to SD.

*Acknowledgements.* This study was supported by the research project Hidrología nival en el Pirineo Central Español: variabilidad espacial, importancia hidrológica y respuesta a la variabilidad y cambio climático (CGL2011-27536/HID, Hidronieve) "CGL2011-27574-CO2-02 and CGL2011-27536, financed by the Spanish Commission of Science and Technology and FEDER; LIFE MEDACC, financed by the LIFE programme of the European Commission"; El glaciar de Monte Perdido: Monitorización y estudio de su dinámica actual y procesos criosféricos asociados como indicadores de procesos de cambio global844/2013,financed by MAGRAMA National Parksand CTTP1/12 "Creación de un modelo de alta resolución espacial para cuantificar la esquiabilidad y la afluencia turística en el Pirineo bajo distintos escenarios de cambio climático", financed by the Comunidad de Trabajo de los Pirineos. The first author is a recipient under the pre-doctoral FPU grant program 2010 (Spanish Ministry of Education Culture and Sports). The third author was the recipient of the postdoctoral grants JAE-DOC043 (CSIC) and JCI-2011-10263 (Spanish Ministry of Science and Innovation). The authors thank Adam Winstral for the use of his algorithm for calculating maximum upwind slope.

## References

Anderton, S. P., White, S. M., and Alvera, B.: Evaluation of spatial variability in snow water equivalent for a high mountain catchment, Hydrol. Process., 18, 435–453, 2004.

Bales, R. C. and Harrington, R. F.: Recent progress in snow hydrology, Rev. Geophys., 33, 1011–1020, 1995.

Barnett, T. P., Adam, J. C., and Lettenmaier, D. P.: Potential impacts of a warming climate on water availability in snow-dominated regions, Nature, 438, 303–309, 2005.

Beale, C. M., Lennon, J. J., Yearsley, J. M., Brewer, M. J., and Elston, D. A.: Regression analysis of spatial data, Ecol. Lett., 13, 246–264, 2010.

Beniston, M.: Climatic change in mountain regions: a review of possible impacts, Climatic Change, 59, 5–31, 2003.

Breiman, L.: Classification and Regression Trees, Wadsworth International Group, Belmont, California, USA, 1984.

Caballero, Y., Voirin-Morel, S., Habets, F., Noilhan, J., LeMoigne, P., Lehenaff, A., and Boone, A.: Hydrological sensitivity of the Adour-Garonne river basin to climate change, Water Resour. Res., 43, W07448, doi:10.1029/2005WR004192, 2007.
Deems, J. S., Fassnacht, S. R., and Elder, K. J.: Fractal distribution of snow depth from Lidar data, J. Hydrometeorol., 7, 285–297, 2006.
Deems, J. S., Fassnacht, S. R., and Elder, K. J.: Interannual consistency in fractal snow depth patterns at two Colorado Mountain sites, J. Hydrometeorol., 9, 977–988, 2008.
Del Barrio, G., Alvera, B., Puigdefabregas, J., and Diez, C.: Response of high mountain landscape to topographic variables: Central Pyrenees, Landscape Ecol., 12, 95–115, 1997.
Egli, L., Jonas, T., Grünewald, T., Schirmer, M., and Burlando, P.: Dynamics of snow ablation in a small Alpine catchment observed by repeated terrestrial laser scans, Hydrol. Process., 26, 1574–1585, 2012.
Elder, K., Dozier, J., and Michaelsen, J.: Snow accumulation and distribution in an Alpine Watershed, Water Resour. Res., 27, 1541–1552, 1991.
Elder, K., Rosenthal, W., and Davis, R. E.: Estimating the spatial distribution of snow water equivalence in a montane watershed, Hydrol. Process., 12, 1793–1808, 1998.
Erickson, T. A., Williams, M. W., and Winstral, A.: Persistence of topographic controls on the spatial distribution of snow in rugged mountain terrain, Colorado, United States, Water Resour. Res., 41, 1–17, 2005.
Erxleben, J., Elder, K., and Davis, R.: Comparison of spatial interpolation methods for estimating snow distribution in the Colorado Rocky Mountains, Hydrol. Process., 16, 3627–3649, 2002.
Fassnacht, S. R. and Deems, J. S.: Measurement sampling and scaling for deep montane snow depth data, Hydrol. Process., 20, 829–838, 2006.
Fassnacht, S. R., Dressler, K. A., and Bales, R. C.: Snow water equivalent interpolation for the Colorado River Basin from snow telemetry (SNOTEL) data, Water Resour. Res., 39, SWC31–SWC310, 2003.
Fassnacht, S. R., López-Moreno, J. I., Toro, M., and Hultstrand, D. M.: Mapping snow cover and snow depth across the Lake Limnopolar watershed on Byers Peninsula, Livingston Island, Maritime Antarctica, Antarct. Sci., 25, 157–166, 2013.
Fu, P. and Rich, P. M.: A geometric solar radiation model with applications in agriculture and forestry, Comput. Electron. Agr., 37, 25–35, 2002.

Groffman, P. M., Driscoll, C. T., Fahey, T. J., Hardy, J. P., Fitzhugh, R. D., and Tierney, G. L.: Colder soils in a warmer world: a snow manipulation study in a northern hardwood forest ecosystem, Biogeochemistry, 56, 135–150, 2001.

Grünewald, T., Schirmer, M., Mott, R., and Lehning, M.: Spatial and temporal variability of snow depth and ablation rates in a small mountain catchment, The Cryosphere, 4, 215–225, doi:10.5194/tc-4-215-2010, 2010.

Grünewald, T., Stötter, J., Pomeroy, J. W., Dadic, R., Moreno Baños, I., Marturià, J., Spross, M., Hopkinson, C., Burlando, P., and Lehning, M.: Statistical modelling of the snow depth distribution in open alpine terrain, Hydrol. Earth Syst. Sci., 17, 3005–3021, doi:10.5194/hess-17-3005-2013, 2013.

Hair, J. F., Anderson, R., Tatham, R., and Black, W.: Multivariate Data Analysis, Printice Hall, Upper Saddle River, New Jersey, USA, 1998.

Hosang, J. and Dettwiler, K.: Evaluation of a water equivalent of snow cover map in a small catchment area using a geostatistical approach, Hydrol. Process., 5, 283–290, 1991.

Jost, G., Weiler, M., Gluns, D. R., and Alila, Y.: The influence of forest and topography on snow accumulation and melt at the watershed-scale, J. Hydrol., 347, 101–115, 2007.

Keller, F., Kienast, F., and Beniston, M.: Evidence of response of vegetation to environmental change on high-elevation sites in the Swiss Alps, Reg. Environ. Change, 1, 70–77, 2002.

Lehning, M., Löwe, H., Ryser, M., and Raderschall, N.: Inhomogeneous precipitation distribution and snow transport in steep terrain, Water Resour. Res., 44, W07404, doi:10.1029/2007WR006545, 2008.

Liston, G. E.: Interrelationships among snow distribution, snowmelt, and snow cover depletion: implications for atmospheric, hydrologic, and ecologic modeling, J. Appl. Meteorol., 38, 1474–1487, 1999.

López-Moreno, J. I. and Nogués-Bravo, D.: A generalized additive model for the spatial distribution of snowpack in the Spanish Pyrenees, Hydrol. Process., 19, 3167–3176, 2005.

López-Moreno, J. I., Latron, J., and Lehmann, A.: Effects of sample and grid size on the accuracy and stability of regression-based snow interpolation methods, Hydrol. Process., 24, 1914–1928, 2010.

López-Moreno, J. I., Vicente-Serrano, S. M., Morán-Tejeda, E., Lorenzo-Lacruz, J., Kenawy, A., and Beniston, M.: Effects of the North Atlantic Oscillation (NAO) on combined temperature and precipitation winter modes in the Mediterranean mountains: observed relationships and projections for the, 21st century, Global Planet. Change, 77, 62–76, 2011.

López-Moreno, J. I., Fassnacht, S. R., Heath, J. T., Musselman, K. N., Revuelto, J., Latron, J., Morán-Tejeda, E., and Jonas, T.: Small scale spatial variability of snow density and depth over complex alpine terrain: implications for estimating snow water equivalent, Adv. Water Resour., 55, 40–52, 2012a.

López-Moreno, J. I., Pomeroy, J. W., Revuelto, J., and Vicente-Serrano, S. M.: Response of snow processes to climate change: spatial variability in a small basin in the Spanish Pyrenees, Hydrol. Process., 27, 2637–2650, 2012b.

McCreight, J. L., Slater, A. G., Marshall, H. P., and Rajagopalan, B.: Inference and uncertainty of snow depth spatial distribution at the kilometre scale in the Colorado Rocky Mountains: the effects of sample size, random sampling, predictor quality, and validation procedures, Hydrol. Process., 28, 933–957, 2014.

Molotch, N. P. and Bales, R. C.: Scaling snow observations from the point to the grid element: implications for observation network design, Water Resour. Res., 41, W11421, doi:10.1029/2005WR004229, 2005.

Molotch, N. P., Colee, M. T., Bales, R. C., and Dozier, J.: Estimating the spatial distribution of snow water equivalent in an alpine basin using binary regression tree models: the impact of digital elevation data and independent variable selection, Hydrol. Process., 19, 1459–1479, 2005.

Mott, R., Schirmer, M., Bavay, M., Grünewald, T., and Lehning, M.: Understanding snow-transport processes shaping the mountain snow-cover, The Cryosphere, 4, 545–559, doi:10.5194/tc-4-545-2010, 2010.

Mott, R., Schirmer, M., and Lehning, M.: Scaling properties of wind and snow depth distribution in an Alpine catchment, J. Geophy. Res.-Atmos., 116, D06106, doi:10.1029/2010JD014886, 2011.

Pomeroy, J. W. and Gray, D. M.: Snowcover Accumulation, Relocation, and Management, National Hydrological Research Institute, Saskatoon, Sask., Canada, 1995.

Pomeroy, J., Essery, R., and Toth, B.: Implications of spatial distributions of snow mass and melt rate for snow-cover depletion: observations in a subarctic mountain catchment, Ann. Glaciol., 38, 195–201, 2004.

Prokop, A.: Assessing the applicability of terrestrial laser scanning for spatial snow depth measurements, Cold Reg. Sci. Technol., 54, 155–163, 2008.





TCD
8, 1937–1972, 2014

Topographic control of snowpack distribution

J. Revuelto et al.

Prokop, A., Schirmer, M., Rub, M., Lehning, M., and Stocker, M.: A comparison of measurement methods: terrestrial laser scanning, tachymetry and snow probing for the determination of the spatial snow-depth distribution on slopes, Ann. Glaciol., 49, 210–216, 2008.

Revuelto, J., López-Moreno, J. I., Azorin-Molina, C., Zabalza, J., Arguedas, G., and Vicente-Serrano, S. M.: Mapping the annual evolution of snow depth in a small catchment in the Pyrenees using the long-range terrestrial laser scanning, J. Maps, 10, 379–393, doi:10.1080/17445647.2013.869268, 2014.

Schaffhauser, A., Adams, M., Fromm, R., Jörg, P., Luzi, G., Noferini, L., and Sailer, R.: Remote sensing based retrieval of snow cover properties, Cold Reg. Sci. Technol., 54, 164–175, 2008.

Schirmer, M. and Lehning, M.: Persistence in intra-annual snow depth distribution: 2. Fractal analysis of snow depth development, Water Resour. Res., 47, W09517, doi:10.1029/2010WR009429, 2011.

Schirmer, M., Wirz, V., Clifton, A., and Lehning, M.: Persistence in intra-annual snow depth distribution: 1. Measurements and topographic control, Water Resour. Res., 47, W09516, doi:10.1029/2010WR009426„ 2011.

Scipión, D. E., Mott, R., Lehning, M., Schneebeli, M., and Berne, A.: Seasonal small-scale spatial variability in alpine snowfall and snow accumulation, Water Resour. Res., 49, 1446–1457, 2013.

Steger, C., Kotlarski, S., Jonas, T., and Schär, C.: Alpine snow cover in a changing climate: a regional climate model perspective, Clim. Dynam., 41, 735–754, 2012.

Trujillo, E., Ramírez, J. A., and Elder, K. J.: Topographic, meteorologic, and canopy controls on the scaling characteristics of the spatial distribution of snow depth fields, Water Resour. Res., 43, W07409, doi:10.1029/2006WR005317, 2007.

Watson, F. G. R., Anderson, T. N., Newman, W. B., Alexander, S. E., and Garrott, R. A.: Optimal sampling schemes for estimating mean snow water equivalents in stratified heterogeneous landscapes, J. Hydrol., 328, 432–452, 2006.

Weiss, A. D.: Topographic Position and Landforms Analysis, ESRI User Conference, San Diego, USA, 2001.

Willmott, C. J.: On the validation of models, Phys. Geogr., 2, 184–194, 1981.

Winstral, A. and Marks, D.: Simulating wind fields and snow redistribution using terrain-based parameters to model snow accumulation and melt over a semi-arid mountain catchment, Hydrol. Process., 16, 3585–3603, 2002.

Winstral, A., Elder, K., and Davis, R. E.: Spatial snow modeling of wind-redistributed snow using terrain-based parameters, J. Hydrometeorol., 3, 524–538, 2002.
Wipf, S., Stoeckli, V., and Bebi, P.: Winter climate change in alpine tundra: plant responses to changes in snow depth and snowmelt timing, Climatic Change, 94, 105–121, 2009.
Zar, J. H.: Biostatistical Analysis, 2nd. edn., Prentice Hall, Englewood Cliffs, New Jersey, USA, 1984.





TCD
8, 1937–1972, 2014

Topographic control of snowpack distribution

J. Revuelto et al.

**Table 1.** Summary statistics of the snowpack distribution and the snow covered area of the basin. Note that snow covered area is expressed as a % of the total area surveyed by the TLS, and the mean SD is the average of all SDs not including zero values.

| | Snow season 2012 | | | | | | Snow season 2013 | | | | | |
|---|---|---|---|---|---|---|---|---|---|---|---|---|
| | 22 Feb | 02 Apr | 17 Apr | 02 May | 14 May | 24 May | 17 Feb | 03 Apr | 25 Apr | 06 Jun | 12 Jun | 20 Jun |
| Mean SD (m) | 0.72 | 0.58 | 0.60 | 0.97 | 0.71 | 0.70 | 2.98 | 3.22 | 2.53 | 2.28 | 2.09 | 1.61 |
| Max SD (m) | 5.5 | 3.8 | 5.3 | 6.1 | 4.4 | 4.3 | 10.9 | 11.2 | 10.1 | 9.6 | 8.9 | 7.9 |
| SCA (%) | 67.2 | 33.5 | 94.1 | 98.8 | 30.9 | 18.9 | 98.8 | 100.0 | 96.3 | 86.4 | 77.1 | 67.0 |





TCD
8, 1937–1972, 2014

**Table 2.** Multiple linear regression beta coefficients for each independent variable and sampled day.

| | Snow season 2012 | | | | | | Snow season 2013 | | | | | |
|---|---|---|---|---|---|---|---|---|---|---|---|---|
| | 22 Feb | 02 Apr | 17 Apr | 02 May | 14 May | 24 May | 17 Feb | 03 Apr | 25 Apr | 06 Jun | 12 Jun | 20 Jun |
| TPI | −0.70 | −0.53 | −0.60 | −0.59 | −0.48 | −0.40 | −0.78 | −0.72 | −0.73 | −0.80 | −0.74 | −0.72 |
| Sx | | 0.11 | 0.28 | 0.26 | 0.20 | 0.16 | 0.36 | 0.31 | 0.43 | 0.37 | 0.38 | 0.31 |
| Elev | 0.09 | 0.22 | 0.34 | 0.27 | 0.27 | 0.35 | | 0.14 | | 0.08 | | 0.13 |
| Slope | | −0.25 | −0.29 | −0.24 | −0.21 | −0.21 | | −0.10 | −0.14 | −0.16 | −0.09 | −0.15 |
| North | −0.22 | 0.13 | −0.16 | | | | −0.12 | −0.11 | −0.11 | | | |
| Curv. | 0.10 | | | | | | 0.29 | 0.25 | 0.25 | 0.31 | 0.23 | 0.20 |
| East | | | | | | 0.06 | 0.12 | 0.08 | | 0.07 | 0.07 | |
| Rad | | | | | | | | | | 0.08 | 0.08 | 0.07 |
| $r^2$ | 0.48 | 0.35 | 0.53 | 0.51 | 0.34 | 0.28 | 0.65 | 0.58 | 0.54 | 0.55 | 0.54 | 0.48 |





TCD
8, 1937–1972, 2014

TCD
8, 1937–1972, 2014



J. Revuelto et al.





**Table 3.** Contribution of the various topographic variables to the explained variance of SD distribution in the binary regression models for 2012 and 2013. Values have been rescaled from 0 to 100.

| | Snow season 2012 | | | | | | Snow season 2013 | | | | | |
|---|---|---|---|---|---|---|---|---|---|---|---|---|
| | 22 Feb | 02 Apr | 17 Apr | 02 May | 14 May | 24 May | 17 Feb | 03 Apr | 25 Apr | 06 Jun | 12 Jun | 20 Jun |
| TPI | 83.1 | 78.0 | 75.0 | 71.7 | 74.0 | 66.9 | 49.1 | 56.4 | 64.4 | 70.0 | 69.7 | 77.6 |
| Sx | | | 4.6 | 12.7 | 13.4 | 10.8 | 45.9 | 23.1 | 23.0 | 23.3 | 20.8 | 12.4 |
| Elev. | 4.7 | 6.5 | 13.2 | 9.1 | 8.2 | 15.2 | 5.0 | 5.7 | 5.0 | 3.3 | 5.3 | 5.4 |
| Slope | 0.9 | 4.4 | 5.7 | 6.5 | 3.2 | 7.0 | | | 2.1 | | | |
| North | 7.3 | 7.6 | 1.5 | | 1.3 | | | 14.7 | 4.3 | | | |
| East | | | | | | | | | 1.2 | 1.2 | 1.1 | 1.5 |
| Rad | 3.8 | 1.2 | | | | | | | | 2.2 | 2.1 | 3.2 |
| $r^2$ | 0.55 | 0.44 | 0.52 | 0.54 | 0.46 | 0.39 | 0.58 | 0.56 | 0.55 | 0.53 | 0.53 | 0.50 |

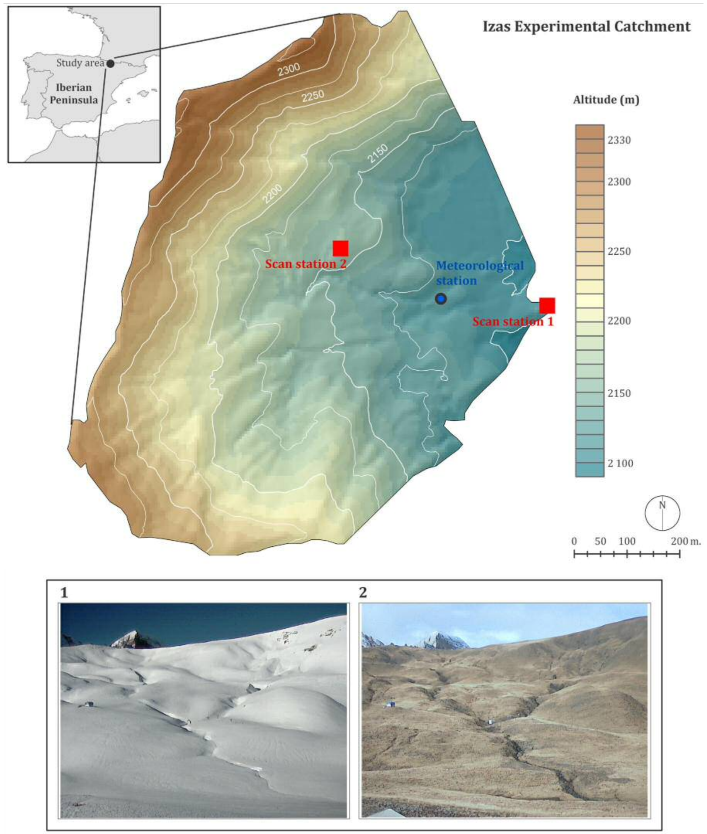


**Fig. 1.** Location of the Izas experimental catchment, and the digital elevation model showing the positions of the scan stations and the automatic meteorological station. The two images in the bottom part of the figure, from Scan Station 1, show the terrain characteristics with (1) and without snow cover (2).





TCD
8, 1937–1972, 2014

Topographic control of snowpack distribution

J. Revuelto et al.

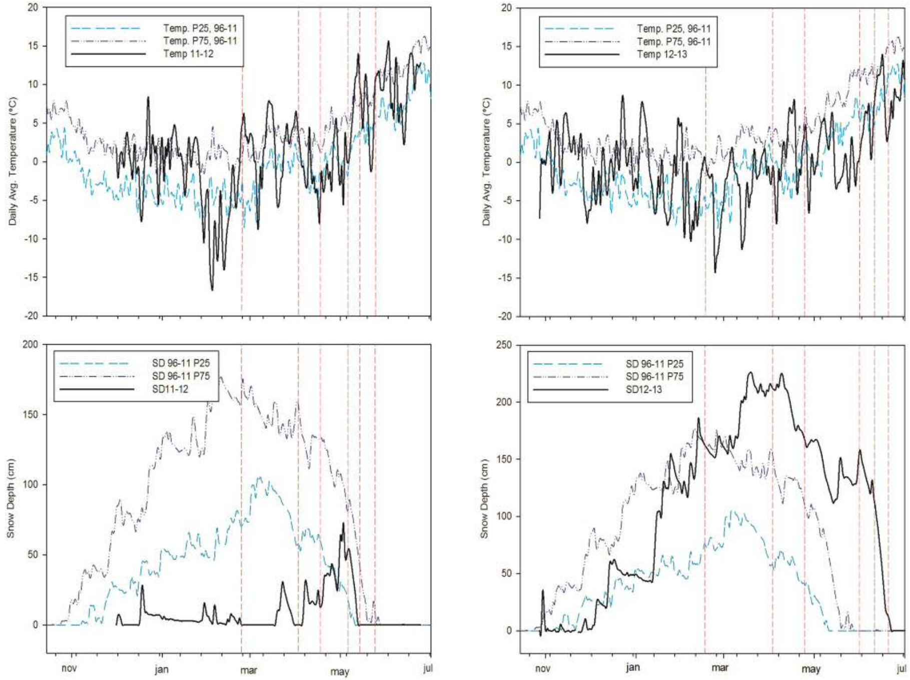


**Fig. 2.** Daily average temperature and snow depth at the automatic weather station (AWS) for the 2012 (left) and 2013 (right) snow seasons. The continuous lines represent the daily values for 2012 and 2013, and the dashed lines show the 25th and 75th percentiles of historical daily series (1996–2011). The vertical dashed lines show the TLS survey days. Note that during some surveys no snow was present at the AWS, but some areas of the Izas experimental catchment were covered by snow.

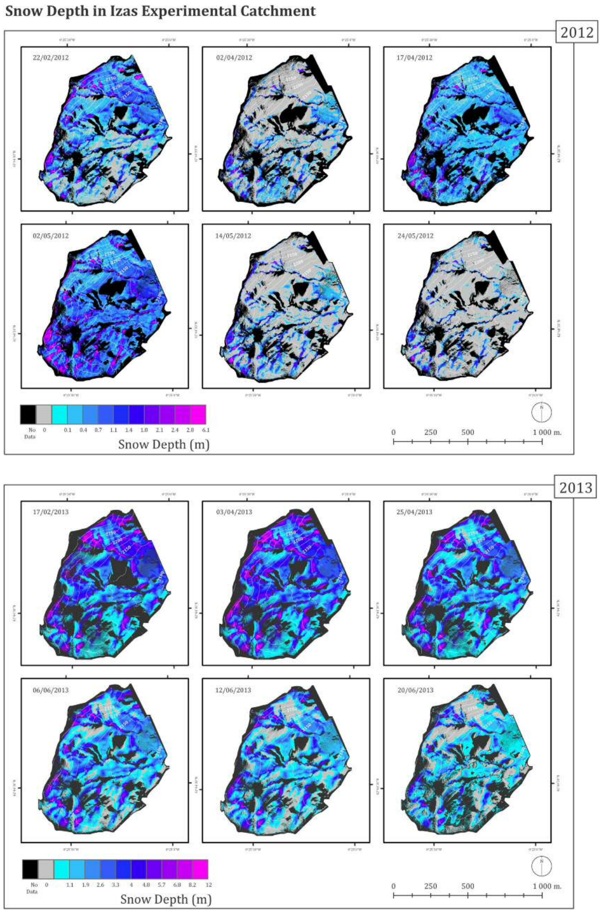


**Fig. 3.** Spatial distribution of snow depth in the Izas experimental catchment in the surveys undertaken in 2012 and 2013.





TCD
8, 1937–1972, 2014

Topographic control of snowpack distribution

J. Revuelto et al.

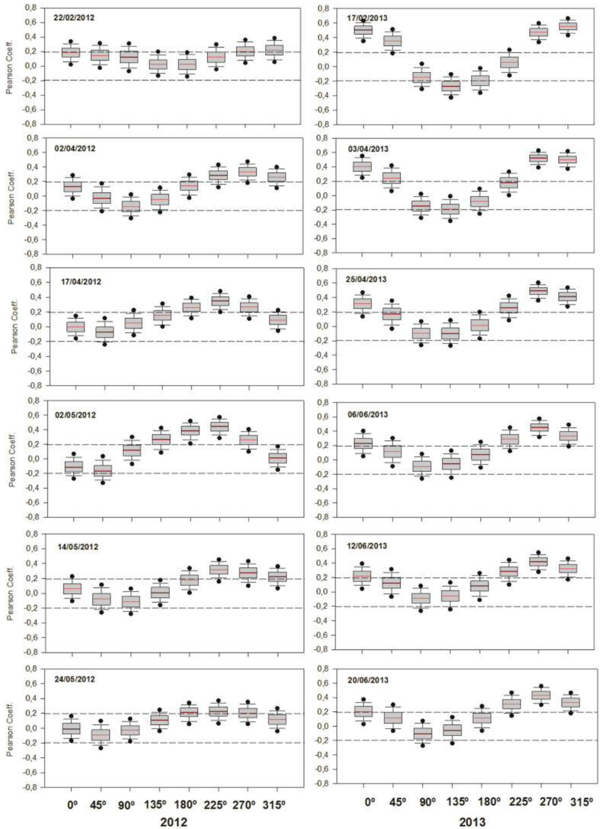


**Fig. 4.** Box plots of the Pearson's *r* coefficients between SD and *Sx*, calculated for the eight studied wind directions over the survey days for the 1000 samples randomly selected following a Monte Carlo approach. The red line shows the mean value, the black continuous line shows the median, the boxes show the 25th and 75th percentile range, the black dots show the 5th and 95th percentiles, and the whiskers show the 10th and 90th percentiles. The dashed lines mark the thresholds for significant correlations ($\alpha < 0.05$).





TCD
8, 1937–1972, 2014

Topographic control of snowpack distribution

J. Revuelto et al.

Title Page
Abstract Introduction
Conclusions References
Tables Figures
◀I ▶I
◀ ▶
Back Close
Full Screen / Esc
Printer-friendly Version
Interactive Discussion

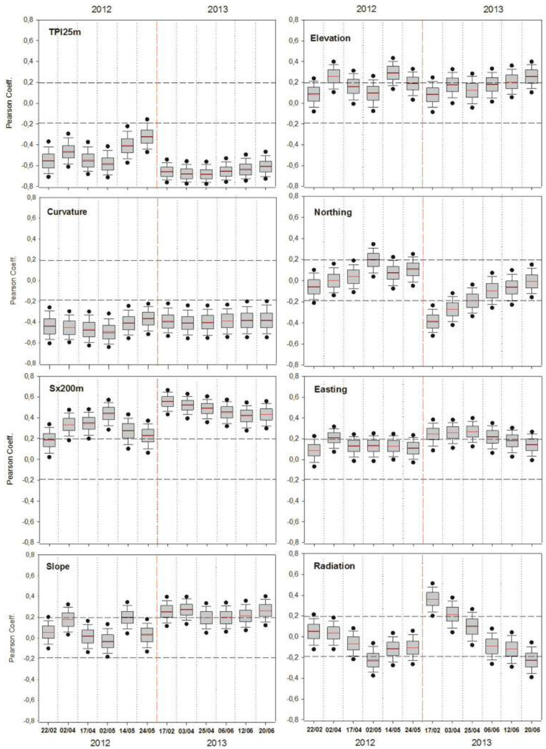


**Fig. 5.** Box plots of the Pearson's $r$ coefficients between SD and the various topographic variables for the 1000 samples randomly selected following a Monte Carlo approach. The red line shows the mean value, the black continuous line shows the median, the boxes show the 25th and 75th percentile range, the black dots show the 5th and 95th percentiles, and the whiskers show the 10th and 90th percentiles. The dashed lines mark the thresholds for significant correlations ($\alpha < 0.05$). Note that the *Sx* coefficients shown in this figure are the preferred *Sx* direction with SD for each day.





TCD
8, 1937–1972, 2014



J. Revuelto et al.

Title Page
Abstract
Introduction
Conclusions
References
Tables
Figures
◀|
|▶
◀
▶
Back
Close
Full Screen / Esc
Printer-friendly Version
Interactive Discussion

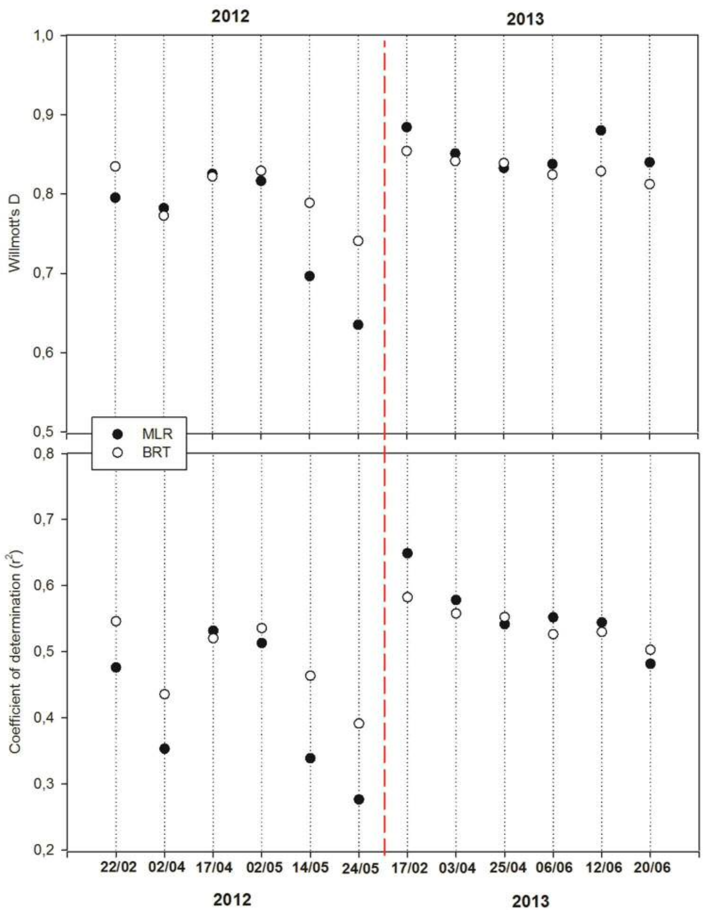


**Fig. 6.** Willmott's $D$ and $r^2$ values between the observed and predicted SD, based on the multiple linear and binary regression models for all survey days.





TCD
8, 1937–1972, 2014

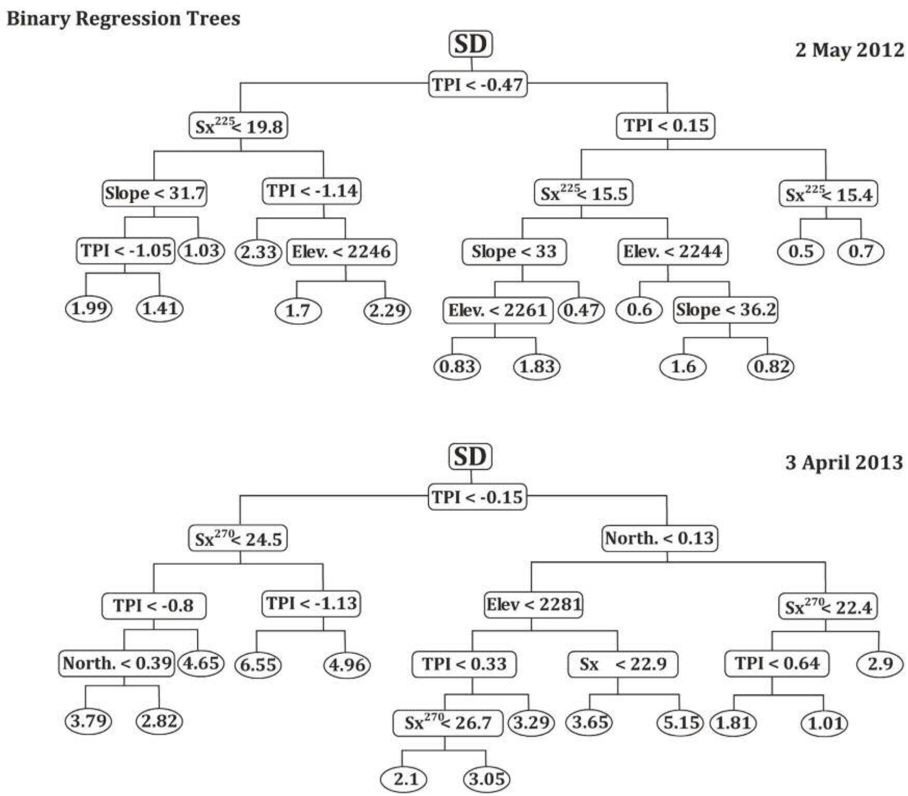


**Fig. 7.** Binary regression tree obtained for 2 May 2012 (top) and 3 April 2013 (bottom). The final nodes (with ellipses) show the predicted SD in the zone having the specified terrain characteristics. At each branch point, one topographic variable is considered; if the value is less than the specified value, the left branch is selected, but if it is equal to or greater than the specified value, the right branch is selected.